Half-life of the yrast 2^+ state in ^{188}W: Evolution of deformation and collectivity in neutron-rich tungsten isotopes

P. J. R. Mason,[1,*] Zs. Podolyák,[1] N. Mărginean,[2] P. H. Regan,[1,3] P. D. Stevenson,[1] V. Werner,[4] T. Alexander,[1] A. Algora,[5,6] T. Alharbi,[1,7] M. Bowry,[1] R. Britton,[1] A. M. Bruce,[8] D. Bucurescu,[2] M. Bunce,[1] G. Căta-Danil,[2] I. Căta-Danil,[2] N. Cooper,[4] D. Deleanu,[2] D. Delion,[2] D. Filipescu,[2] W. Gelletly,[1] D. Ghiţă,[2] I. Gheorghe,[2] T. Glodariu,[2] G. Ilie,[4] D. Ivanova,[9] S. Kisyov,[9] S. Lalkovski,[9] R. Lica,[2] S. N. Liddick,[10] R. Mărginean,[2] C. Mihai,[2] K. Mulholland,[11,12] C. R. Nita,[2] A. Negret,[2] S. Pascu,[2] S. Rice,[1] O. J. Roberts,[8] T. Sava,[2] J. F. Smith,[11,12] P.-A. Söderström,[13] L. Stroe,[2] G. Suliman,[2] R. Suvaila,[2] S. Toma,[2] C. Townsley,[1] E. Wilson,[1] R. T. Wood,[1] M. Zhekova,[9] and C. Zhou[4]

[1]*Department of Physics, University of Surrey, Guildford, Surrey GU2 7XH, United Kingdom*
[2]*Horia Hulubei National Institute of Physics and Nuclear Engineering (IFIN-HH), RO-077125 Bucharest, Romania*
[3]*National Physical Laboratory, Teddington, Middlesex TW11 0LW, United Kingdom*
[4]*Wright Nuclear Structure Laboratory, Yale University, New Haven, Connecticut 06520, USA*
[5]*IFIC, CSIC-Universitat de Valencia, Apartado Oficial 22085, 46071 Valencia, Spain*
[6]*MTA ATOMKI, 4001 Debrecen, Pf. 51, Hungary*
[7]*Department of Physics, College of Science in Zulfi, Almajmaah University, P.O. Box 1712, 11932, Saudi Arabia*
[8]*School of Computing, Engineering and Mathematics, University of Brighton, Brighton BN2 4GJ, United Kingdom*
[9]*Department of Physics, University of Sofia, 1164 Sofia, Bulgaria*
[10]*National Superconducting Cyclotron Laboratory (NSCL), Michigan State University, East Lansing, Michigan 48824, USA*
[11]*University of the West of Scotland, Paisley PA1 2BE, United Kingdom*
[12]*Scottish Universities Physics Alliance (SUPA), University of Glasgow, Glasgow, United Kingdom*
[13]*RIKEN Nishina Center for Accelerator Based Science, Hirosawa, Wako, Saitama 351-0198, Japan*

(Received 27 February 2013; revised manuscript received 18 July 2013; published 2 October 2013)

The half-life of the yrast $I^\pi = 2^+$ state in the neutron-rich nucleus ^{188}W has been measured using fast-timing techniques with the HPGe and LaBr$_3$:Ce array at the National Institute of Physics and Nuclear Engineering, Bucharest. The resulting value of $t_{1/2} = 0.87(12)$ ns is equivalent to a reduced transition probability of $B(E2; 2_1^+ \to 0_1^+) = 85(12)$ W.u. for this transition. The $B(E2; 2_1^+ \to 0_1^+)$ is compared to neighboring tungsten isotopes and nuclei in the Hf, Os, and Pt isotopic chains. Woods-Saxon potential energy surface (PES) calculations have been performed for nuclei in the tungsten isotopic chain and predict prolate deformed minima with rapidly increasing γ softness for $^{184-192}$W and an oblate minimum for ^{194}W.

DOI: 10.1103/PhysRevC.88.044301 PACS number(s): 21.10.Tg, 23.20.Lv, 27.70.+q

I. INTRODUCTION

The ground states of nuclei in the $A \sim 190$ region of the nuclear chart around $70 \leqslant Z \leqslant 78$ are predicted to undergo shape transitions from prolate to oblate quadrupole deformation with increasing neutron number in a variety of theoretical works [1–4]. Recent theoretical calculations of deformation in this region [5–7] suggest a sharper transition from axially deformed prolate to axially deformed oblate in the lower Z (Yb, Hf) nuclei than in the higher-Z isotopic chains which are predicted to become increasingly γ soft or have triaxial ground states. The $N = 118$ isotope, ^{196}Pt displays one of the best empirical examples of the $O(6)$ dynamical symmetry, corresponding to a flat nuclear potential in the γ degree of freedom [8]. In the W and Os isotopic chains, γ softness is predicted to reach a maximum at $N = 116$ [7] and a minimum in the experimental γ-vibrational band-head energy, $E(2_2^+)$, is observed at ^{192}Os$_{116}$, suggesting that it is the most γ-unstable Os isotope [7].

In the tungsten isotopes, a systematic increase in yrast $I^\pi = 2^+$ energy and decrease in $E(4_1^+)/E(2_1^+)$ is observed as one moves from stable to neutron-rich isotopes [9]. Tungsten isotopes with $N \leqslant 112$ have a value of $E(4_1^+)/E(2_1^+)$ close to 3.3, the limit for a perfect axial rotor. The decrease in $E(4_1^+)/E(2_1^+)$ for heavier isotopes indicates a deviation from rigid axial symmetry. This is compatible with increasing γ softness and possibly the beginning of the shape phase transition towards oblate-deformed ground states [7,10]. However, a sharp deviation in the ratio of $4^+/2^+$ energies from the systematic trend has been reported in ^{190}W and it has been suggested that this may be evidence for the emergence of a subshell closure at $Z = 76$ in this region [10]. Measurement of the reduced transition probability, $B(E2; 2_1^+ \to 0_1^+)$, is a good indicator of the ground state collectivity of a nucleus and half-life measurements are expected to give insight into the structure of nuclei in this transitional region.

In the present work, we report on a measurement of the half-life of the yrast $I^\pi = 2^+$ state in the neutron-rich isotope, $^{188}_{74}$W$_{114}$. The experiment employed fast-timing techniques with the LaBr$_3$:Ce scintillator and high-purity germanium (HPGe) detector array [11] at the National Institute of Physics and Nuclear Engineering (IFIN-HH), Bucharest. Excited states

*Present address: STFC Daresbury Laboratory, Daresbury, Warrington, WA4 4AD, UK.

in ^{188}W have previously been investigated using multinucleon transfer reactions [12,13] and β-delayed spectroscopy [9] which found the structure to be consistent with an increased γ softness and decreased quadrupole moment compared to the stable W isotopes.

II. EXPERIMENT AND DATA ANALYSIS

Excited states in ^{188}W were populated using the ^{186}W(^{7}Li,αp)^{188}W reaction, where the reaction mechanism is thought to be a combination of incomplete fusion and low-energy transfer. The ^{7}Li beam was accelerated to 31 MeV by the Tandem van de Graaff accelerator at IFIN-HH, Bucharest and impinged on a 16 mg/cm^2 enriched ^{186}W target with a 43 mg/cm^2 lead backing. The population of ^{188}W for this reaction was estimated to be ~0.5% of the total γ-γ statistics for the reaction with the strongest channels being the ^{186}W(^{7}Li,$\alpha 2n$)^{187}Re and ^{186}W(^{7}Li,$4n$)^{189}Ir reactions. The experiment ran for ~218 h, during which the average beam intensity on target was ~4 particle-nA. Gamma rays produced in the reaction were detected with an array of eight HPGe detectors and 11 LaBr$_3$:Ce detectors. Data were recorded when the master trigger condition, that coincident γ rays were observed in $\geqslant$2 LaBr$_3$:Ce detectors and $\geqslant$1 HPGe detector or in $\geqslant$3 HPGe detectors, was met.

The HPGe and LaBr$_3$:Ce detectors were calibrated in energy using ^{152}Eu and ^{60}Co sources. The energy dependence of the time response ("time walk") of the LaBr$_3$:Ce detectors was determined with a ^{60}Co source using the method described in Ref. [11] in which the time response of each detector is fitted with a polynomial function and corrected down to ~100 keV in offline analysis. The half-lives of excited states populated in the reaction were measured by extracting the time difference between γ rays observed in pairs of LaBr$_3$:Ce detectors. The timing information in each LaBr$_3$:Ce detector was recorded relative to the master trigger and the time difference between any two detectors was found by subtracting their times relative to the trigger as described in Ref. [11]. Three-dimensional $E_{\gamma 1}$-$E_{\gamma 2}$-ΔT histograms (cubes) were constructed in such a way that the time difference between two transitions can be obtained by gating on their photopeaks on the energy axes of the cube [11].

The HPGe detectors were used to set γ-ray energy coincidence conditions that selected a particular γ-ray cascade within the LaBr$_3$:Ce spectra. The high resolution of the HPGe detectors makes it possible to resolve weaker γ-ray transitions and create clean LaBr$_3$:Ce $E_{\gamma 1}$-$E_{\gamma 2}$-ΔT cubes for the more weakly produced isotopes by requiring a particular transition to be observed in coincidence in the HPGe detectors. Figure 1 shows the spectrum resulting from gating on the 143-keV, $2^+ \to 0^+$ transition of ^{188}W. The energies of other previously reported transitions in this nucleus [12] are marked on the figure. The inset in Fig. 1 shows the partial level scheme for ^{188}W relevant to this work, adapted from Ref. [12].

III. RESULTS

In such fast timing experiments, the half-life of a state is ideally measured from the time difference between transitions directly feeding and depopulating it. However, due to the weak population of ^{188}W relative to other reaction channels in the present work, it was not possible to obtain a time-difference

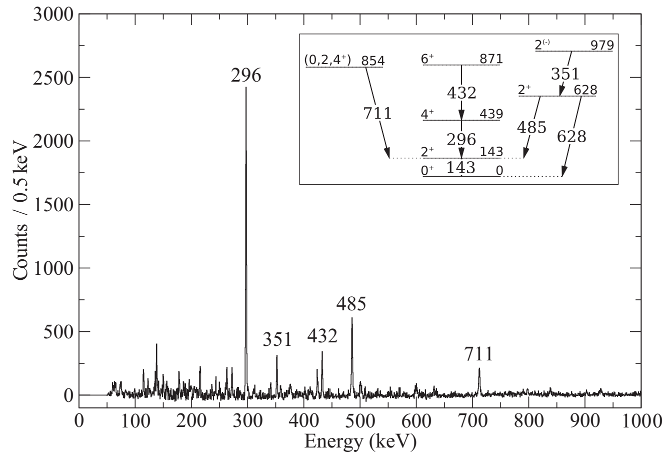

FIG. 1. HPGe γ ray spectrum in coincidence with the 143-keV transition detected in the HPGe detectors. Peaks belonging to ^{188}W [12] are labeled by their energies in keV. The inset shows a partial level scheme for ^{188}W relevant to this work, adapted from Ref. [12].

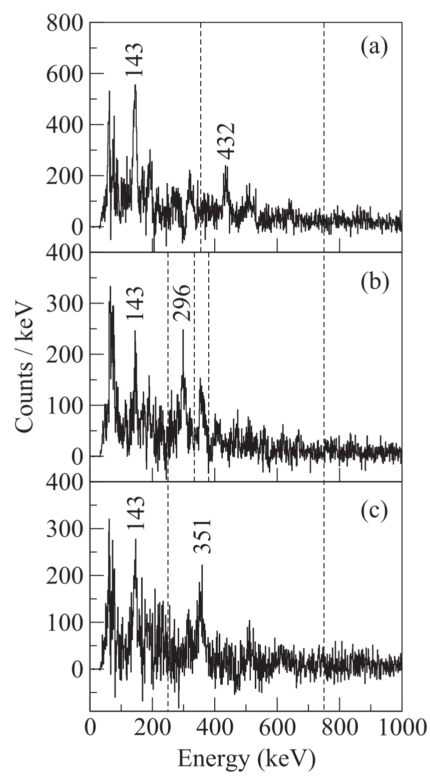

FIG. 2. LaBr$_3$:Ce γ-ray spectra in coincidence with the (a) 296-keV, (b) 432-keV, and (c) 485-keV transitions detected in the HPGe detectors. Peaks belonging to ^{188}W [12] are labeled by their energies in keV. The regions inside the dashed lines were used as "start" gates for the time difference spectra. Note that areas of strong contamination, such as the peak at ~350 keV in (b) were rejected from these gates (see text for details).

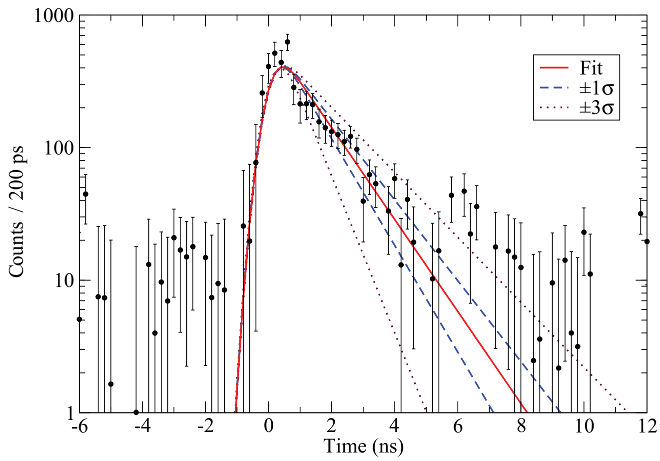

FIG. 3. (Color online) Time spectrum for the decay of the yrast 2^+ state in ^{188}W measured from the time difference between the 143-keV transition and all observed feeding transitions (see text for details). The solid line represents a fit to the data giving a half-life of $t_{1/2} = 0.87(12)$ ns. The dashed and dotted lines represent 1σ and 3σ deviations in the half-life, respectively.

spectrum with sufficient statistics to determine the half-life of the yrast 2^+ state.

To maximize the available statistics, HPGe gates were set on the observed 296-, 432-, and 485-keV transitions which feed the yrast 2^+ state to create three $LaBr_3$:Ce $E_{\gamma 1}$-$E_{\gamma 2}$-ΔT cubes. The HPGe gates were background subtracted in energy but still show some contamination from other γ rays produced in the reaction. However, the 143-keV transition is uncontaminated in each of the resulting $LaBr_3$:Ce spectra, which are shown in Fig. 2.

The time difference was measured between the photopeak of the 143-keV transition depopulating the 2^+ state and a region of the $LaBr_3$:Ce spectra from 250- to 750-keV. This continuous region will contain the photopeaks and Compton-scattered γ rays of any transition feeding the yrast 2^+ state and higher lying states in ^{188}W. Strong contaminant photopeaks and regions where the background was oversubtracted (due to contamination in the HPGe background gates) were excluded from the gate, as shown in Fig 2, to minimize possible contamination in the final time-difference spectra. However, after two clean, background-subtracted gates on the 143-keV transition and one other ^{188}W transition, contamination of the resulting time spectra is assumed to be negligible. The three time-difference spectra were summed together to create the spectrum shown in Fig. 3.

As the time-difference in Fig. 3 is effectively between the 143-keV transition and any other ^{188}W γ ray populated in the reaction, the observed time difference will also partially depend on the half-lives of any intermediate states in the feeding of the yrast 2^+ state. Due to the limited spin and excitation energy imparted by the reaction, the states important in this feeding are the yrast 4^+ state at an excitation energy of 439 keV and the second 2^+ state at 628 keV [12]. The half-lives of these states are assumed to be much shorter and thus negligible compared to that of the yrast 2^+ state and so the time-difference spectrum in Fig. 3 is assumed to be solely representative of the yrast 2^+ half-life. This assumption can be shown to be reasonable by comparison with ^{186}W, in which the measured half-lives of the yrast 4^+ and the second 2^+ state state are 36.4(25) ps and 4.78(16) ps, respectively [14]. The half-lives of the equivalent states in ^{188}W can be expected to be of the same order-of-magnitude. The estimated range of these half-lives for the feeding states has been included in the final uncertainty for the half-life of the yrast 2^+ state.

The time spectrum was fitted with a convolution between an exponential decay and the Gaussian time resolution of the detector array, from which the half-life of the yrast 2^+ state in ^{188}W was measured to be $t_{1/2} = 0.87(12)$ ns. The full-width at half maximum (FWHM) and $\Delta T = 0$ centroid of the Gaussian were fixed from fits to the decay of the yrast 2^+ state in ^{190}Os [15]. ^{190}Os was populated with high statistics out of beam from the electron-capture decay of ^{190}Ir in the target activity at the end of the experiment and the time difference measured between the 187- and 361-keV transitions. In fits to the ^{190}Os time difference spectrum, all parameters of the convolution, including the FWHM and centroid, were allowed to vary freely. The ^{190}Os yrast 2^+ half-life was measured to be $t_{1/2} = 375(20)$ ps [15], in excellent agreement with the literature value of $t_{1/2} = 375(10)$ ps [16].

IV. DISCUSSION

The present half-life measurement of $t_{1/2} = 0.87(12)$ ns corresponds to a reduced transition probability for ^{188}W of

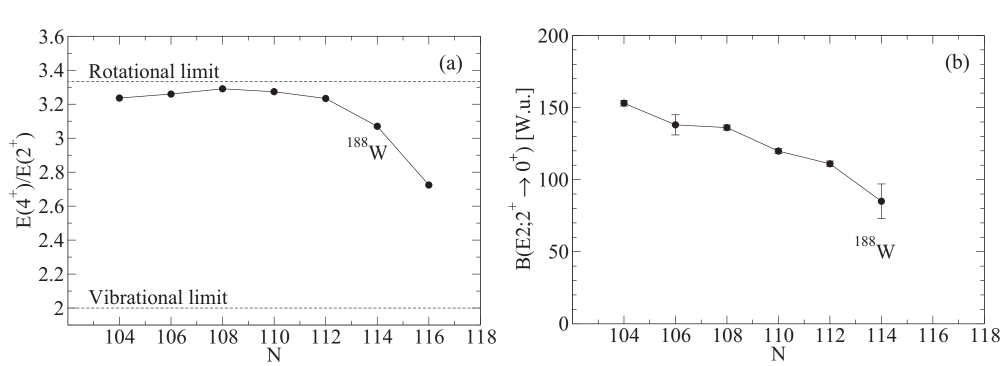

FIG. 4. Experimental values of (a) $E(4_1^+)/E(2_1^+)$ and (b) $B(E2; 2_1^+ \to 0_1^+)$ in even-A tungsten isotopes. The data are taken from the Nuclear Data Sheets [14,16,19–23] except the $B(E2; 2_1^+ \to 0_1^+)$ for ^{178}W [24]. The $B(E2; 2_1^+ \to 0_1^+)$ for ^{188}W is from this work.

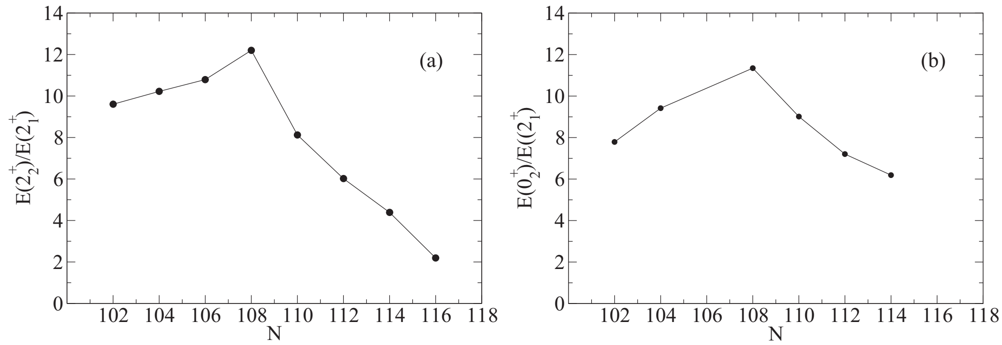

FIG. 5. Experimental values of (a) $E(2_2^+)/E(2_1^+)$ and (b) $E(0_2^+)/E(2_1^+)$ in even-A tungsten isotopes. The data are taken from the Nuclear Data Sheets [14,16,19–23] except the $E(2_2^+)$ in ^{190}W, which is taken from Ref. [9]. The 886-keV level in ^{188}W is assumed to be the 0_2^+.

$B(E2; 2_1^+ \rightarrow 0_1^+) = 5.46(75) \times 10^3\ e^2\text{fm}^4$ which is equivalent to $B(E2; 2_1^+ \rightarrow 0_1^+) = 85(12)$ W.u. Figure 4 shows the systematics of $B(E2; 2_1^+ \rightarrow 0_1^+)$ values and $E(4_1^+)/E(2_1^+)$ in the even W isotopes. ^{188}W appears to display a larger decrease in $B(E2; 2_1^+ \rightarrow 0_1^+)$ compared to the systematic trend of lighter W isotopes, similar to the decrease in $E(4_1^+)/E(2_1^+)$ observed for ^{188}W. However, the uncertainty in the present measurement means that the data point could represent a continuation of the approximately linear trend for the isotopic chain. As such, this information alone does not indicate whether ^{188}W marks the beginning of a prolate-oblate shape change in this region or simply represents a smooth continuation in the decreasing collectivity as the closed neutron shell at $N = 126$ is approached.

Figure 5 shows $E(2_2^+)/E(2_1^+)$ and $E(0_2^+)/E(2_1^+)$ energy ratios for even-A tungsten isotopes. The 2_2^+ and 0_2^+ levels are assumed to be the γ and β vibrational band heads, respectively, and the excitation energy of these states indicates the susceptibility of the nuclear shape to changes in γ or β deformation (i.e., γ or β softness). Both ratios reach a maximum at ^{182}W ($N = 108$) indicating that this nucleus has the most rigid nuclear shape of any W isotope. $E(4_1^+)/E(2_1^+)$ also maximises at ^{182}W, where it is very close to the rigid-rotor limit of $3.\dot{3}$. $E(2_2^+)/E(2_1^+)$ decreases rapidly for W isotopes with $N > 108$ which is consistent with increasing γ softness approaching $N = 116$.

Figure 6 shows the systematics of $E(4_1^+)/E(2_1^+)$ and $B(E2; 2_1^+ \rightarrow 0_1^+)$ for even W isotopes along with those for neighboring even-even nuclei in the Hf, Os, and Pt isotopic chains. Ignoring smaller variations, the trend in $B(E2; 2_1^+ \rightarrow 0_1^+)$ for all these nuclei is a linear decrease with increasing neutron number. The $B(E2; 2_1^+ \rightarrow 0_1^+)$ value does not maximize at the neutron midshell ($N = 104$) in any of these isotopic chains as might be expected in a simplistic interacting-boson description where collectivity is highest for the largest number of valence nucleons.

The $E(4_1^+)/E(2_1^+)$ ratio shows a more complex dependence on both N and Z. The Pt isotopes shown in Fig. 6 all have $E(4_1^+)/E(2_1^+)$ ratios close to the asymptotic limit for a γ soft nucleus of ~2.5 (though such a ratio can arise from a range of structures with the IBM triangle) [17]. The W and Os chains evolve away from the limit of a rigid axial rotor as neutron number is increased. The $E(4_1^+)/E(2_1^+)$ ratios seem to agree with the predictions of the potential energy surface (PES) calculations in Ref. [5], which predict a smoother evolution in shape for the higher-Z isotopic chains and that the γ degree of freedom to plays a more important role in the Os and Pt isotopes.

To estimate the ground-state deformations for even-A W isotopes from $^{184-194}$W, potential energy surface (PES) calculations were performed for this work and are shown in Fig. 7. The calculations employed a nonaxial deformed

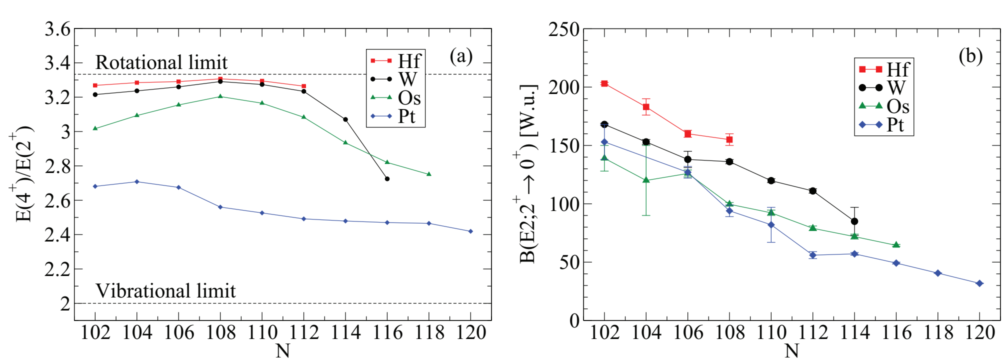

FIG. 6. (Color online) Experimental (a) $E(4_1^+)/E(2_1^+)$ and (b) $B(E2; 2_1^+ \rightarrow 0_1^+)$ values in even-A Hf, W, Os, and Pt isotopes. Data points are taken from Nuclear Data Sheets [14,16,19–23,25–30] except the $B(E2; 2_1^+ \rightarrow 0_1^+)$ for ^{174}Hf, ^{176}W [31], and ^{178}W [24]. The $B(E2; 2_1^+ \rightarrow 0_1^+)$ for ^{188}W is from the current work.

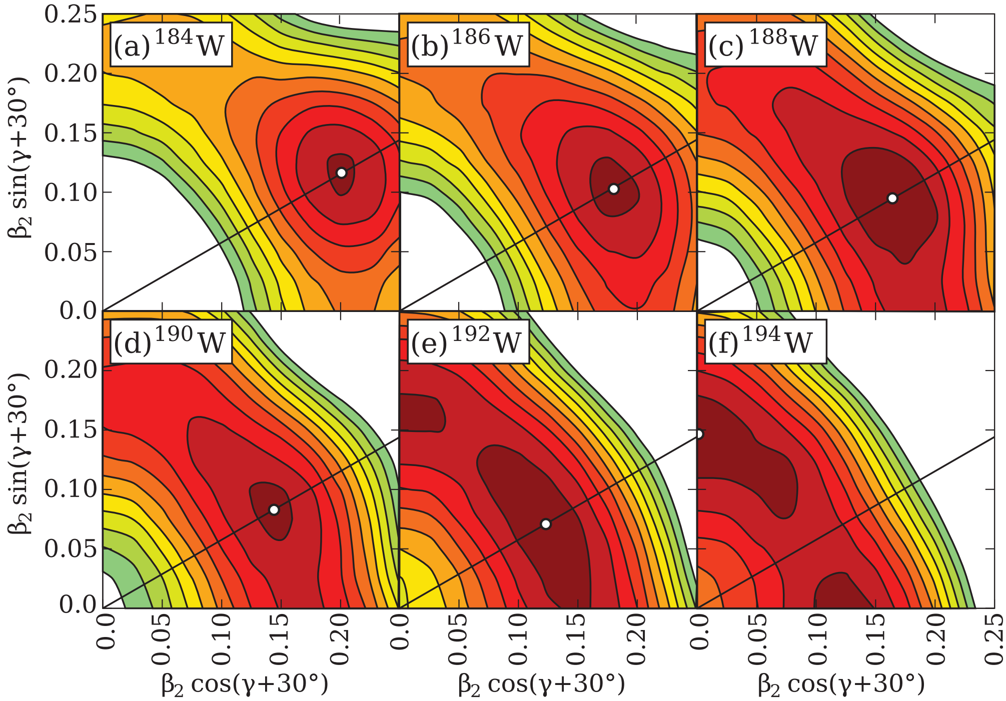

FIG. 7. (Color online) Potential energy surface calculations for the ground-state configurations of even-A tungsten isotopes. The white dots indicate the minima of the surfaces and the contours are separated by 400 keV.

Woods-Saxon potential and for each point in β_2 and γ, the potential energy is minimized as a function of hexadecapole deformation, β_4. In contrast to the calculations in Ref. [5], these calculations do not predict triaxial minima for the ground states of any W isotopes. In the present calculations, the minima are predicted to remain prolate for $^{184-192}$W, but become increasingly γ soft with increasing neutron number. The minimum for ^{194}W is predicted to have an oblate, γ soft minimum. The surfaces of ^{192}W and ^{194}W have both prolate and oblate minima and are almost flat with respect to the triaxial degree of freedom, close to the type of surface expected for the $O(6)$ symmetry [8].

The PES calculations predict a ground state quadrupole deformation of $\beta_2 = 0.190$ with significant γ softness for ^{188}W. The increased γ softness for the ^{188}W PES compared to the stable W isotopes ^{184,186}W is consistent with the decrease in $E(4_1^+)/E(2_1^+)$ and $B(E2; 2_1^+ \to 0_1^+)$ observed experimentally. The transition quadrupole moment for ^{188}W can be extracted from the $B(E2; 2_1^+ \to 0_1^+)$ under the assumption that it is an axially deformed rotating nucleus [18]. The present measurement gives $|Q_t| = 5.2(4)$ eb. For a good rotor, the transition quadrupole moment can be considered to be equal to the intrinsic quadrupole moment, $|Q_0|$, and an estimate of the effective quadrupole deformation parameter, $|\beta_{2,\mathrm{eff}}|$ can be obtained. Assuming a uniform charge distribution, a value of $|\beta_{2,\mathrm{eff}}| = 0.18(1)$ is obtained for ^{188}W, which is consistent with the minimum at $\beta_2 = 0.190$ found in the PES calculations.

V. SUMMARY

In conclusion, the present measurement of $t_{1/2} = 0.87(12)$ ns for the half-life of the yrast 2^+ state in ^{188}W corresponds to $B(E2; 2_1^+ \to 0_1^+) = 85(12)$ W.u. This appears to show a sharper decrease in collectivity compared to the trend of lighter tungsten isotopes, albeit with a relatively large error. This implies a possibly increased γ softness for ^{188}W compared to stable tungsten isotopes in agreement with the expectations for this mass region [1,2,5]. The decrease is similar to that observed in the ratio of energies, $E(4_1^+)/E(2_1^+)$ for the W isotopic chain. Potential energy surface calculations in this work predict prolate minima with increasing γ softness for heavier W isotopes and an oblate minimum for ^{194}W.

The measured half-life and other bulk observables discussed in this work do not give an unambiguous picture of the structure of neutron-rich W nuclei. However, they demonstrate a deviation from rigid axial symmetry and are compatible with the beginning of the widely predicted [1–7] prolate-to-oblate shape transition in neutron-rich W isotopes. Measurements in heavier isotopes are required to determine the exact nature of the structural evolution in this region.

ACKNOWLEDGMENTS

We would like to thank the staff of IFIN-HH, Romania for their support during this experiment and Professor R. Wadsworth for the loan of the ^{186}W target. This work was supported by the Science and Technology Facilities Council, STFC(UK), Engineering and Physical Sciences Research Council, EPSRC(UK), The Romanian Ministry for Education and Research [contracts no. PN-II-ID-PCE-2011-3-0367(UEFISCDI) and PN 09 37 01 05 (NuSTAR)], ANCS(Romania), The Spanish Ministerio de Educación y Ciencia under Grant No. FPA2011-24553, Bulgarian Science

Fund contract no. DMU02/1, Bulgarian-Romanian Partnership contract nos. BRS-07/23 and 460/PNII Module III, and the US DoE under Grant No. DE-FG02-91ER-40609. T.A. acknowledges the support of Almajmaah University, Saudi Arabia. P.A.S. acknowledges the support of the Japan Society for the Promotion of Science (JSPS) Kakenhi Grant No. 23·01752. P.H.R. also acknowledges partial support from the Yale University Flint Fund.

[1] W. Nazarewicz, M. A. Riley, and J. D. Garrett, Nucl. Phys. A **512**, 61 (1990).
[2] R. Bengtsson, T. Bengtsson, J. Dudek, G. Leander, W. Nazarewicz, and J. Z. Zhang, Phys. Lett. B **183**, 1 (1987).
[3] J. Jolie and A. Linnemann, Phys. Rev. C **68**, 031301(R) (2003).
[4] P. D. Stevenson, M. P. Brine, Z. Podolyak, P. H. Regan, P. M. Walker, and J. R. Stone, Phys. Rev. C **72**, 047303 (2005).
[5] L. M. Robledo, R. Rodríguez-Guzmán, and P. Sarriguren, J. Phys. G **36**, 115104 (2009).
[6] K. Nomura, T. Otsuka, R. Rodríguez-Guzmán, L. M. Robledo, and P. Sarriguren, Phys. Rev. C **84**, 054316 (2011).
[7] K. Nomura *et al.*, Phys. Rev. C **83**, 054303 (2011).
[8] J. A. Cizewski, R. F. Casten, G. J. Smith, M. L. Stelts, W. R. Kane, H. G. Borner, and W. F. Davidson, Phys. Rev. Lett. **40**, 167 (1978).
[9] N. Alkhomashi *et al.*, Phys. Rev. C **80**, 064308 (2009).
[10] Zs. Podolyák *et al.*, Phys. Lett. B **491**, 225 (2000).
[11] N. Mărginean *et al.*, Eur. Phys. J. A **46**, 329 (2010).
[12] T. Shizuma *et al.*, Eur. Phys. J. A **30**, 391 (2006).
[13] G. J. Lane *et al.*, Phys. Rev. C **82**, 051304(R) (2010).
[14] C. M. Baglin, Nucl. Data Sheets **99**, 1 (2003).
[15] P. J. R. Mason *et al.*, AIP Conf. Proc. **1491**, 93 (2012).
[16] B. Singh, Nucl. Data Sheets **99**, 275 (2003).
[17] R. F. Casten, D. D. Warner, D. S. Brenner, and R. L. Gill, Phys. Rev. Lett. **47**, 1433 (1981).
[18] A. Bohr and B. M. Mottelsson, *Nuclear Structure* (Benjamin, New York, 1975), Vol. 2, p. 45.
[19] E. Achterberg, O. A. Capurro, and G. V. Marti, Nucl. Data Sheets **110**, 1473 (2009).
[20] S.-c. Wu and H. Niu, Nucl. Data Sheets **100**, 483 (2003).
[21] B. Singh and J. C. Roediger, Nucl. Data Sheets **111**, 2081 (2010).
[22] C. M. Baglin, Nucl. Data Sheets **111**, 275 (2010).
[23] B. Singh, Nucl. Data Sheets **95**, 387 (2002).
[24] M. Rudigier, J.-M. Régis, J. Jolie, K. O. Zell, and C. Fransen, Nucl. Phys. A **847**, 89 (2010).
[25] E. Browne and H. Junde, Nucl. Data Sheets **87**, 15 (1999).
[26] M. S. Basunia, Nucl. Data Sheets **107**, 791 (2006).
[27] C. M. Baglin, Nucl. Data Sheets **84**, 717 (1998).
[28] B. Singh, Nucl. Data Sheets **107**, 1531 (2006).
[29] H. Xiaolong, Nucl. Data Sheets **108**, 1093 (2007).
[30] H. Xiaolong, Nucl. Data Sheets **110**, 2533 (2009).
[31] J.-M. Régis *et al.*, Nucl. Instrum. Methods Phys. Res. A **606**, 466 (2009).